Geophysical Research Letters

Supporting Information for

Determination of dust aerosol particle size at Gale Crater using REMS UVS and Mastcam measurements

Álvaro Vicente-Retortillo[1,2], Germán M. Martínez[2], Nilton O. Renno[2], Mark T. Lemmon[3] and Manuel de la Torre-Juárez[4]

[1]Departamento de Física de la Tierra, Astronomía y Astrofísica II, Universidad Complutense de Madrid, Madrid, Spain

[2]Department of Climate and Space Sciences and Engineering, University of Michigan, Ann Arbor, Michigan, USA.

[3]Department of Atmospheric Sciences, Texas A&M University, College Station, Texas, USA

[4]Jet Propulsion Laboratory, California Institute of Technology, Pasadena, California, USA.

Contents of this file

Introduction

This supporting information consists of three text segments and three figures to illustrate our methodology to retrieve dust aerosol particle size (Figure S1), to describe our Monte-Carlo radiative transfer model (Text S1), to validate our Monte-Carlo radiative transfer model (Text S2 and Figure S2), to show further evidence of the seasonal variability of dust aerosol particle size (Figure S3) and to list the sources of uncertainties in our results (Text S3).

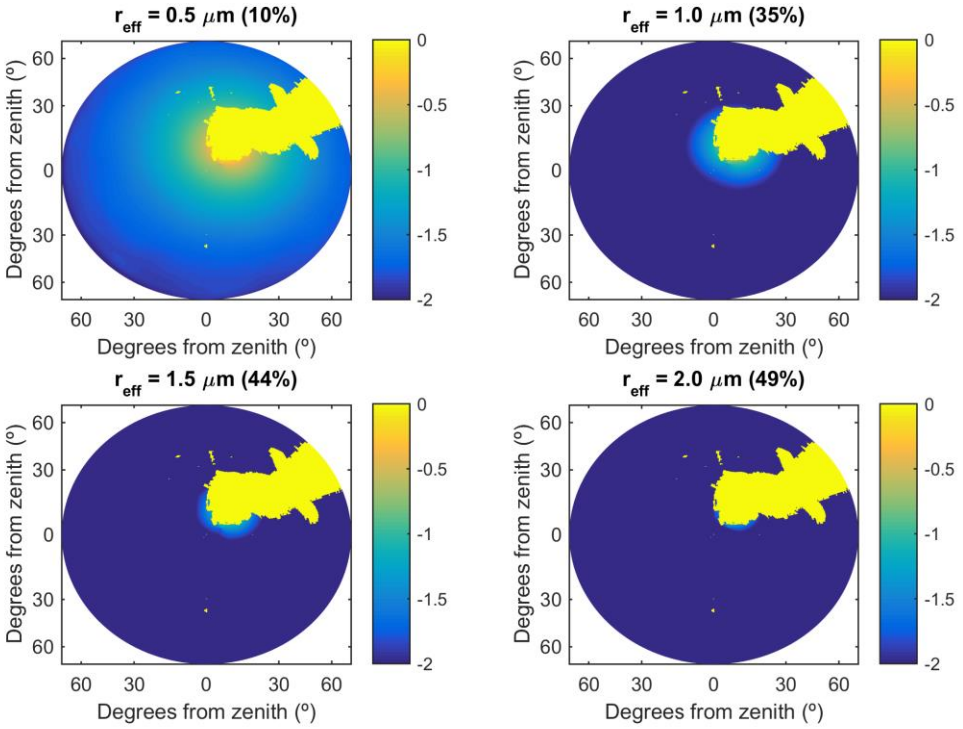

Figure S1. Simulated radiances at 11:29:06 LMST (central point of a shadow event) on sol 775 of the MSL mission considering the empirically derived field of view of the REMS UVE channel for four different values of dust aerosol effective radius. The radiance values are shown in logarithmic scale using color code, and are normalized by the maximum value of the scattered radiance field (for example, a value of -1 indicates that the radiance at that cell is 10^{-1} times the radiance at the cell containing the peak value). For comparison purposes, only radiances above 1% (value of -2) of the peak value are plotted, and regions where radiances are below this threshold are shown in dark blue. The blocked region of the FOV is shown in yellow. The region in which radiances are above 1% of the maximum value decreases with increasing effective radius: for an effective radius of 0.5 μm (top left), this region covers virtually the entire hemisphere, whereas for an effective radius of 2 μm (bottom right) this region is virtually confined within the blocked region of the FOV. Thus, the relative increase in the blocked fraction of scattered radiation with respect to the situation at the limit of the shadow event (when the Sun is very close to the edge of the blocked region of the FOV) increases significantly with effective radius, as quantified in parenthesis in the title of each panel (from 10% with r_{eff} = 0.5 μm to 49% with r_{eff} = 2 μm).

Text S1. The Monte-Carlo radiative transfer model: Description

Solar fluxes on the Martian surface can be directly simulated with modest computational effort using radiative transfer models which, despite their relative simplicity, can provide accurate results [*Vicente-Retortillo et al.*, 2015]. However, since the incoming radiation that is blocked by the masthead and the mast of the rover as a function of particle size is the key quantity in our study, a model capable of calculating radiances is needed. This is why we use our Monte-Carlo radiative transfer model, which calculates radiances by simulating photons' trajectories as a function of optical depth. Since these trajectories are not simulated as a function of height, knowledge of the dust vertical profile is not necessary. Aerosols are assumed to be well mixed, with no variations in single scattering albedo and phase function as a function of optical depth.

At each scattering event, a fraction of the photons (which depends on the single scattering albedo) is absorbed, and then photons are fractionated and scattered in all directions, and these fractions are calculated according to the selected phase function. After performing the simulations, radiances at the surface are stored in lookup tables as a function of opacity, dust effective radius and solar zenith angle (see Section 2).

Text S2. The Monte-Carlo radiative transfer model: Validation

We have calculated radiances under six scenarios using our Monte-Carlo model and DISORT [*Stamnes et al.*, 1988]. Each scenario is defined by selecting a value of dust opacity (0.5, 1 or 1.5), along with a single scattering albedo and a phase function with asymmetry factor corresponding to dust effective particle radii of 1.5 or 1 μm. We have compared the radiances obtained with the two models for each scenario as a function of zenith angle, concluding that they are in excellent agreement. Among the three selected opacities, the largest mean relative departures were found for τ = 1. For the two scenarios with τ = 1, mean relative departures of 1.4% when r_{eff} = 1.5 μm and of 0.95% when r_{eff} = 1 μm are obtained after averaging the absolute values of the relative departures of the radiances within 20º of the solar disk as a function of zenith angle.

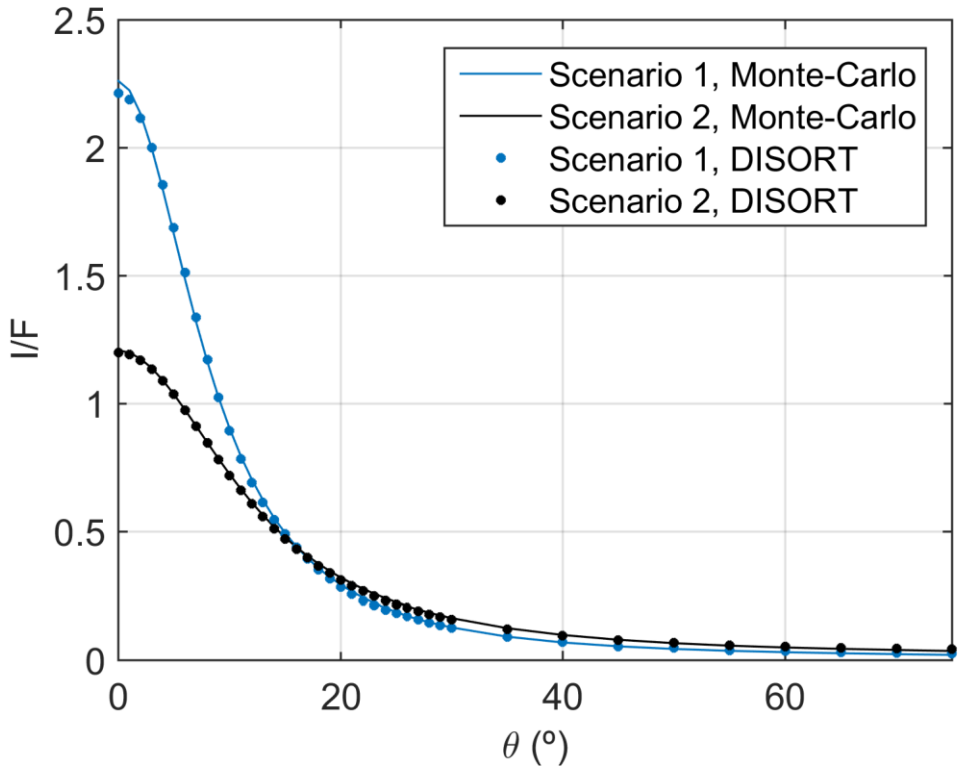

Figure S2. Intensities normalized by the total flux as a function of zenith angle when τ = 1 and r_{eff} = 1.5 μm (scenario 1, blue) and when τ = 1 and r_{eff} = 1 μm (scenario 2, black), using our Monte-Carlo model (solid lines) and DISORT (circles). The agreement between the two models is excellent.

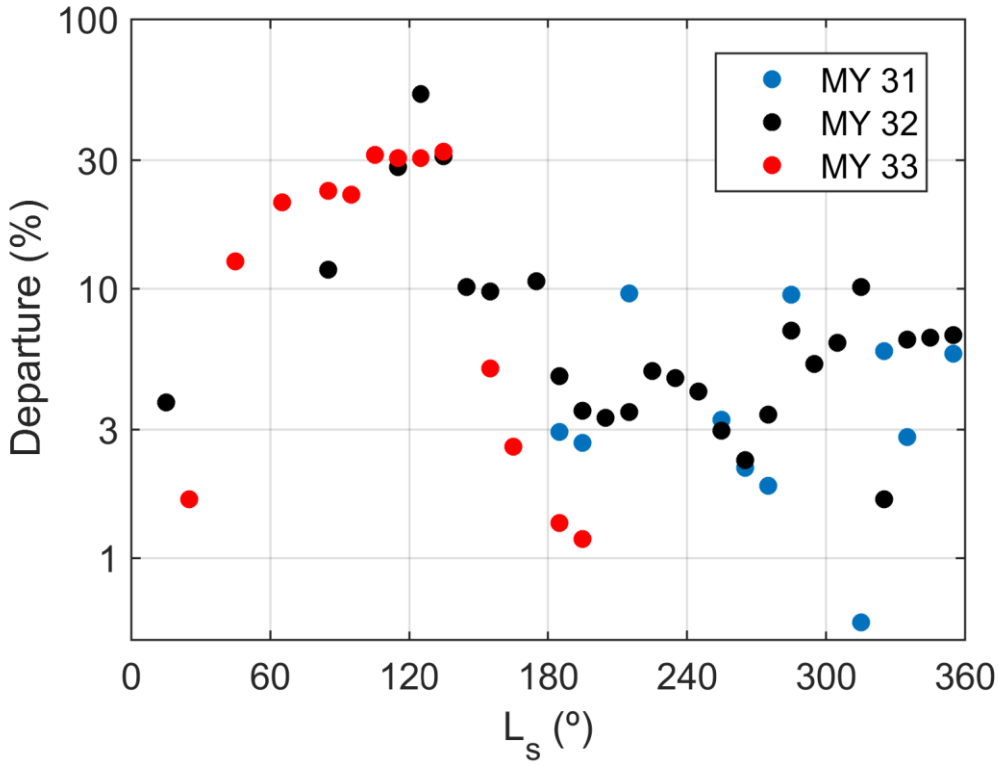

Figure S3. Departures of observed ratios between output currents during shadow events from ratios simulated assuming a constant effective radius of 1.5 μm. Colors as in Figure 2. Departures below 3% are found at solar longitudes when the effective radius is close to 1.5 μm (see Figure 2, top). In contrast, departures around 30% are found during the low opacity season at L_s ~ 120º, when retrieved effective radii are the smallest (~0.6 μm).

Text S3. Uncertainties

In addition to the quantitative analyses of the uncertainties associated to dust and water ice contents performed in Section 2.4, in this section we list and comment additional sources of uncertainties in our results. Quantifications of the effect of each of these additional sources are subject to a large number of free parameters that cannot be straightforwardly constrained. Moreover, the combined effect depends on each particular measurement of each shadow event. To be conservative, we have discarded shadow events in which the uncertainty in the retrieved radius was estimated to be above 0.2 μm. These sources of uncertainties are:

a) Observations: The original requirements of REMS photodiodes were to provide UV fluxes (ENVRDR products) with an accuracy better than 10% with respect to maximum expected values [*Gómez-Elvira et al.*, 2014]. The uncertainties in the fluxes are mainly caused by inaccuracies in the angular response calibration function and by the effects of dust deposited on the sensor, and the noise in the output currents is virtually negligible. As mentioned in Section 2, uncertainties associated to inaccuracies in the angular response are mitigated by using the output currents (TELRDR products) and our empirical angular response function. Similarly, uncertainties associated to dust deposition are mitigated by calculating the ratios of measurements performed during shadow events. Since the duration of these events typically ranges from a few minutes to 1 or 2 hours, the

impact of dust attenuation on each single measurement is assumed to be constant and thus cancel out when taking the ratio of such measurements.

b) Radiative transfer model: Biases in simulated radiances using our Monte-Carlo model are small (see Figure S2). Simulated radiances are also affected by the aerosol vertical distribution. We have assumed that aerosols are well mixed, which is a valid assumption in the absence of water ice clouds.

c) Empirical model of the angular response: Uncertainties in the angular response can be associated with modeling results and with the features of the sensor. Uncertainties in modeling results are caused by uncertainties in the radiances simulated with the Monte-Carlo model. This implies that the empirically derived angular response may differ slightly from the actual response, but it allows a consistent conversion from simulated radiances to output currents, which is very important in order to obtain reliable results. There is also an uncertainty associated to azimuthal variations in the spatial response. These variations are typically small for small solar zenith angles, but increase for zenith angles larger than 30º-40º. This uncertainty is mitigated by selecting measurements that were performed in a short period of time (with small variations in Sun position). Thus, any inaccuracy in the angular response will be compensated when calculating the ratios of the output currents. For this reason, we have only selected shadow events with solar zenith angles smaller than 30º or with solar zenith angles typically between 30º and 40º but with a relative change in the angular response smaller than a 15%.

d) Radiative parameters: Phase functions and single scattering albedos present uncertainties associated with the refractive indices (which could be subject to temporal variations caused by changes in dust composition) and with the assumed particle shape (cylinders) and size distribution (monomodal). Since the actual properties of the Martian dust are not well known, our selection is performed to optimize consistency with the selected refractive indices. There is a well-known discrepancy between the simulated and the observed phase functions in the backscatter direction, but our retrievals are mainly affected by the behavior of the phase function for small scattering angles, where the agreement between simulated and experimental phase functions is very good [*Wolff et al.*, 2010]. Uncertainties in opacity (mainly because Mastcam observations do not coincide in time with REMS shadow events) can also slightly affect the results, as shown in Table 1. Finally, a significant presence of water ice clouds can also affect the results, as quantified in Section 2.4.